Talanta Open 5 (2022) 100087

Contents lists available at ScienceDirect

Talanta Open

journal homepage: www.sciencedirect.com/journal/talanta-open

Nano-molecularly imprinted polymers for serum creatinine sensing using the heat transfer method

Rhys J. Williams [a], Robert D. Crapnell [a], Nina C. Dempsey [a], Marloes Peeters [b], Craig E. Banks [a,*]

[a] Faculty of Science and Engineering, Manchester Metropolitan University, Chester Street, Manchester M1 5GD, United Kingdom
[b] School of Engineering, Newcastle University, Merz Court, Newcastle upon Tyne NE1 7RU, United Kingdom

ARTICLE INFO

Keywords:
Serum creatinine sensing
Solid-phase templating
Nano-molecularly imprinted polymer
Heat transfer method

ABSTRACT

Serum creatinine concentration is an important clinical measure of kidney function. However, standard methods of detection, such as the Jaffe method or enzymatic assays, suffer several disadvantages, including non-specificity and procedural complexity, or high cost, respectively. In this work, we propose the use of nano-molecularly imprinted polymers (nMIPs) in conjunction with the novel Heat Transfer Method (HTM) as a promising alternative sensing platform to these existing methods for measuring serum creatinine concentration. More specifically, it is shown that creatinine-imprinted nMIPs can be produced using a solid-phase templating method, and that simple drop-casting onto a cheap, disposable substrate can be used in conjunction with HTM to detect creatinine with a limit-of-detection of (7.0 ± 0.5) μM in buffer solutions. Furthermore, the nMIPs are shown to selectively bind creatinine in comparison to several similar molecules, and the sensing platform is demonstrated to be able to detect changes in creatinine concentration in complex blood plasma samples.

1. Introduction

Creatinine is a small molecule waste product formed in the body by non-enzymatic dehydration of creatine [1], which is an important biomolecule for vertebrate muscle function [2]. Creatinine is filtered from blood plasma by the kidneys, and subsequently excreted from the body during urination [1]. Due to the molecule's small size and physiologically inert behaviour, it is freely filtered by the kidneys, and hence measurement of creatinine concentration in serum has long been used in clinical settings as a means of assessing a patient's renal function, specifically as an indicator of glomerular filtration rate [1, 3]; simply put, higher-than-normal creatinine concentrations in the blood can indicate kidney disease or injury. While healthy serum creatinine concentrations show significant inter- and intra-individual variations, [3, 4] serum creatinine measurements nonetheless remain important clinical indicators of kidney injury. For example, the British Medical Journal (BMJ) best practice guide suggests that acute kidney injury is indicated by an increase in serum creatinine concentration of $\geq$0.03 mM over 48 hrs, or an increase to $\geq$1.5X the baseline value within 7 days [5].

Serum creatinine concentration is generally measured using either Jaffe or enzymatic assays [6, 7]. The Jaffe method relies on the reaction of creatinine with picrate to produce a quantifiable colour change, whereas enzymatic assays produce a colorimetric response through successive enzymatic reactions [6]. A significant disadvantage of the Jaffe method is its lack of specificity; a variety of common biological compounds can react with picrate and interfere with the conversion of the creatinine chromogen [6, 7]. Additionally, the reaction is somewhat complex to perform since picric acid is a significant chemical hazard, and the reaction is sensitive to temperature and pH. [7] Compared to the Jaffe method, enzymatic assays have higher specificity and sensitivity towards creatinine and hence are used when higher precision is required [6]. However, the use of enzymes is associated with its own drawbacks, not least relatively higher cost and more complex transportation and storage logistics (because enzymes must be stored at low temperatures). A possible means of avoiding many of the drawbacks of either method is to measure creatinine concentration using molecularly imprinted polymers (MIPs) as the recognition element.

The term MIP is used to refer to a cross-linked polymer which has been synthesised in the presence of a template molecule. In the pre-polymer mixture for non-covalent MIPs, molecules of monomer associate with the template via various types of non-covalent, intermolecular bonding, and these structures are subsequently fixed upon polymerisation and cross-linking. Removal of the template molecule, for example through washing, leaves vacancies that will bind the template with a

* Corresponding author.
E-mail address: c.banks@mmu.ac.uk (C.E. Banks).

https://doi.org/10.1016/j.talo.2022.100087
Received 20 October 2021; Received in revised form 18 January 2022; Accepted 22 January 2022
Available online 23 January 2022

high degree of specificity due to their complementary sizes, shapes, and functionalities. Exposing the evacuated MIP to a solution containing the template leads to rebinding in the vacancies, which can be measured using a variety of different sensing methods, including optical [8], gravimetric [9], and electrochemical[10] techniques. While the selective binding of a target molecule by a MIP is analogous to that of the antibodies and enzymes frequently used in sensing, MIPs have a number of advantages in comparison to their biological counterparts. Proteins and enzymes are produced through expensive and complex methodologies, require the utilisation of animals, and rapidly denature outside their tolerated temperature and pH ranges. By contrast, MIPs can be derived from simple and wide-ranging synthetic routes using low-cost feedstocks and have significantly enhanced thermal and chemical stabilities. These advantages mean that there has already been significant interest in the use of MIPs for biomolecule sensing [10–12].

The relatively simple criteria for the formation of MIPs mean that a large variety of synthetic methods have been reported for their production [13]. Processes which can produce MIP nanoparticles (i.e. nano-MIPs, or nMIPs), are especially useful since the extremely high surface-area-to-volume ratio of nanoparticles means that significantly more binding sites are available for interaction with the analyte in nMIPs than in micro- or macro-sized MIPs [14]. A range of syntheses have been reported for nMIPs [14], but they produce particles of varying quality. The ideal nMIP for sensing would have: a high degree of binding site heterogeneity, thereby maximising their sensitivity and specificity towards the target; minimal excess polymer per binding site; and minimal residual template remaining in the material [15]. The procedure reported by Canfarotta et al. addresses these criteria by using a solid-phase templating approach [15]. More specifically, they anchored a target analyte molecule on a glass bead support, and subsequently carried out free radical polymerisation in solution containing the templated glass beads. While polymer nanoparticles formed both at the bead surface and in solution, they found that they could selectively retrieve nMIPs through a temperature gradient washing process, which left the desired particles on the glass bead surface until the final washing step (by which point the unwanted particles had been removed) [15]. Their synthesis could be carried out in both aqueous and organic solvents, and as such allowed them produce monodisperse nMIPs with a high degree of affinity for a range of different targets, including biological macromolecules, as well as small molecules [15].

For creatinine specifically, a range of MIP syntheses have been reported, including emulsion free radical polymerisation to form MIP microparticles [16], sol-gel formation of a creatinine-imprinted aluminosilicate [17], and free radical polymerisation to graft MIPs from a magnetic iron nanoparticle core [18]. The MIP microparticles in particular were demonstrated to form part of an effective sensing platform using Electrochemical Impedance Spectroscopy; the other cited examples demonstrate the binding and selectivity of the synthesised MIPs, but do not establish a sensing platform. To the best of our knowledge, there has been no report of creatinine-imprinted nMIPs made using the procedure described by Canfarotta et al. [15]. Similarly, there has been no report of a sensing platform consisting of creatinine-imprinted MIPs and a thermal method of analysis.

A novel read-out platform for detection of analyte binding to MIPs is the Heat Transfer Method (HTM), which has been shown to be effective when used in conjunction with nMIPs made via the Canfarotta method [19]. This technique relies on the change in the thermal resistance of functional material, such as a nMIP, when it is exposed to the appropriate analyte solution [20]. More specifically, in a typical HTM measurement, a thermocouple is used to measure the temperature of a liquid-filled sample cell while it is being heated by an external heat sink and maintained at a constant temperature by an electric heater and proportional-integral-derivative (PID) controller. The temperature of the solution (T_2), the temperature of the heat sink (T_1), and the power being drawn by the heater (P) are measured continuously, and together they can be used to calculate the thermal resistance (R_{th}) of the system: [20]

$$R_{th} = \frac{T_1 - T_2}{P} \quad (1)$$

A MIP layer can be placed between the heat source and the T_2 thermocouple, typically on a substrate at the bottom of the sample chamber, or as a coating on the thermocouple itself. An illustration of the set-up used in this work is shown in Fig. 1. When analyte is introduced to the solution, it will bind to the nMIP layer and reduce heat flux through it [20]. This in turn reduces the measured T_2 and increases the calculated R_{th}. The increase in R_{th} is dependant on the analyte concentration, typically following a nonlinear relationship which can be calibrated using standards of known concentration and a fitted nonlinear function. Changes in R_{th} in response to changing analyte concentrations can be measured not only in simple aqueous solutions, but also in complex, real biological samples such as serum[19] and plasma [21]. This proven versatility, coupled with the simplicity of HTM systems and the low cost of their components, means that HTM represents a promising alternative to traditional clinical sensing methods, including, in theory, clinical evaluation of serum creatinine concentrations.

In this paper, we report for the first time, a simplified version of the synthetic approach developed by Canfarotta et al. [15]. to produce nMIPs imprinted for creatinine which are effective recognition elements for sensing of serum creatinine using HTM. The nMIPs are first characterised using a variety of analytical methods and are then shown to measure creatinine in aqueous buffer solutions using the HTM. The nMIPs are shown to be selective for creatinine sensing in comparison to chemically similar interferent molecules and are then finally demonstrated to provide a measurable response in real blood plasma. Overall, it is concluded that the concept of serum creatinine sensing using nMIPs in conjunction with HTM is promising, although both the nMIP synthesis and HTM system would require further optimisation before being useful in a clinical setting.

2. Experimental section

2.1. Materials

Details of all materials used in this work are given in the Supporting Information (SI).

2.2. nMIPs synthesis

The synthetic methodology used here was taken from Canfarotta et al., [15] but with some simplifications. Firstly, while Canfarotta et al. suggest the use of a cocktail of monomers in order to provide correct functionality for binding to target analytes, [15] only one monomer, N-isopropylacrylamide (NIPAM), and cross-linker, N,N'-methylenebisacrylamide (BIS), were used herein. This is because it was predicted that the amide groups on these molecules would provide sufficient non-covalent interactions with creatinine to cause molecular imprinting; the obtained nMIPs are therefore expected to be largely composed of poly(N-isopropylacrylamide) (PNIPAM). The chemical structures of creatinine, NIPAM, and BIS are shown in Fig. 2 for reference. Additionally, while Canfarotta et al. describe an uncontrolled radical polymerisation for their aqueous nMIPs synthesis, an iniferter agent, 2-(2-Carboxyethylsulfanylthiocarbonylsulfanyl)propionic acid, (CTP, also shown in Fig. 2) was used here to provide controlled/living free radical polymerisation. This is because living free radical polymerisation has been shown to improve the homogeneity of binding sites within MIPs compared to uncontrolled polymerisation [22], and should promote the formation of monodisperse particle sizes [15]. Finally, while Canfarotta et al. suggest reaction in organic solvent for imprinting small molecules, and aqueous synthesis when using biological macromolecules, an aqueous synthesis was used here despite creatinine being a small molecule since it was found to be significantly more soluble in

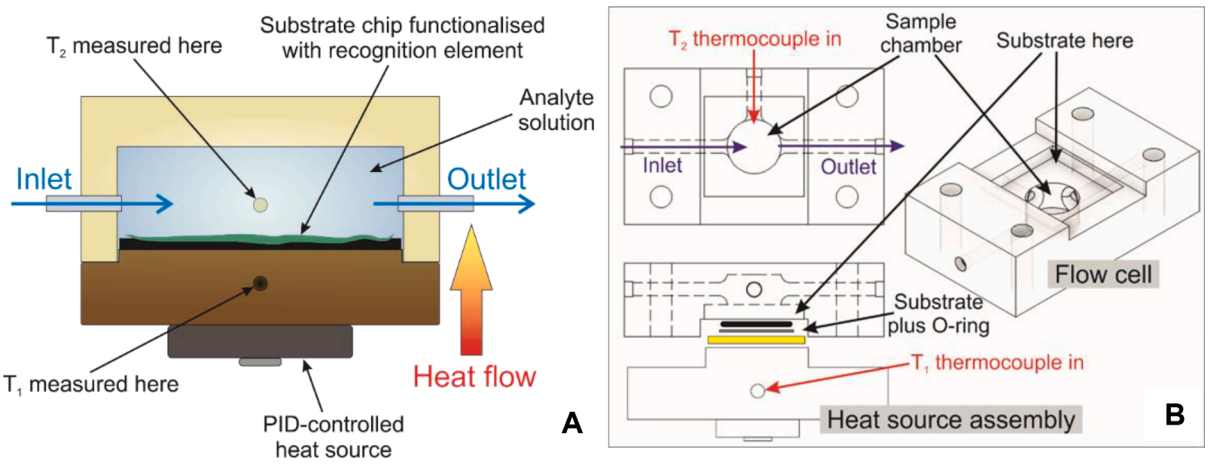

Fig. 1. An illustration of the basic set-up used for HTM measurements in this work, with (A) showing a cartoon representing the assembled flow cell during a measurement, and (B) showing part drawings for the individual components of the disassembled flow cell.

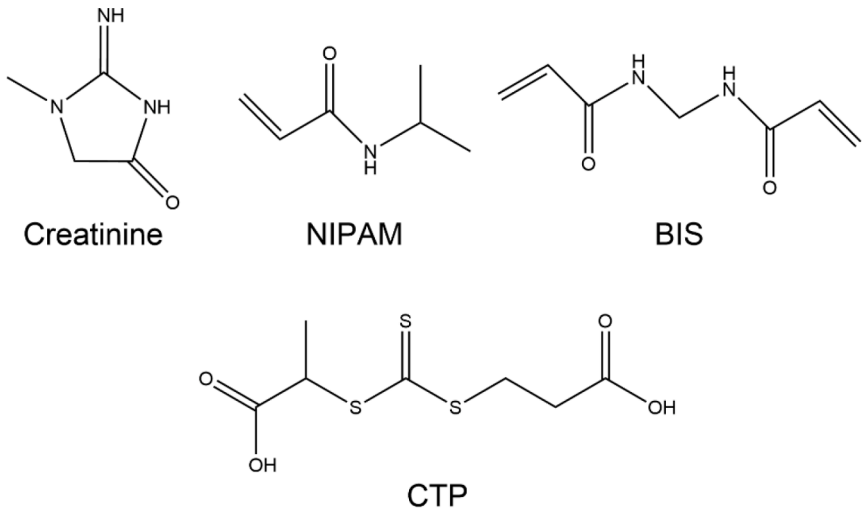

Fig. 2. Chemical structures of creatinine, N-isopropylacrylamide (NIPAM), N,N'-methylenebisacrylamide (BIS), and 2-(2-Carboxyethylsulfanylthiocarbonylsulfanyl) propionic acid (CTP).

water than organic solvents [15].

An abridged summary of the synthetic procedure is as follows, with the full, unabridged version given in the SI:

Part 1 – glass bead activation and amine coating: the glass beads were activated by reflux in 1 M sodium hydroxide then washed to neutral pH using 0.01 M phosphate-buffered saline (PBS) solution and deionised water. After being fully dried in an oven, the activated beads were coated with (3-Aminopropyltrimethoxy)silane by overnight reaction in toluene under dry conditions. The coated beads were then washed with acetone and methanol and then dried in air.

Part 2 – creatinine template attachment: the dry coated beads were treated for 2 hrs at ambient temperature with a solution of glutaraldehyde (7% v/v) in 0.01 M PBS, before being filtered and rinsed with deionised water. The glutaraldehyde-treated beads were then added to a 45 mM solution of creatinine in 0.01 M PBS and left in a fridge overnight. The creatinine solution was then decanted and replaced with a solution of sodium borohydride in deionised water (approximately 1 $mgmL^{-1}$). After 30 min reaction at ambient temperature, the beads were retrieved by filtration then rinsed with deionised water and dried in air.

Part 3 – nMIP synthesis on templated glass beads: in deionised water, NIPAM, CTP, and BIS were dissolved to give a molar ratio of approximately 26:18:1, respectively. The solution was purged with N_2 (g) before the addition of the creatinine-templated glass beads, which was followed by further purging. Finally, ammonium persulfate and N,N,N′,N′-Tetramethylethylenediamine were mixed in a molar ratio of 1:1.25, respectively, then quickly added to monomer solution to initiate polymerisation, with the mixture then left to react for 24 hrs under inert atmosphere and at ambient temperature.

Part 4 – nMIP collection: after reaction, the polymerisation mixture was decanted into a solid-phase extraction tube fitted with a poly (ethylene) frit. This was used to rinse the beads with eight 30 mL aliquots of deionised water at room temperature which removed unwanted reactants and non-imprinted polymer nanoparticles; all but the last of these aliquots were discarded (the final aliquot was kept for analysis). In order to retrieve the desired nMIPs, a 30 mL aliquot of deionised water at 60 °C was then added to the beads and left for 15 min before being collected and stored. This was repeated three times to yield 90 mL of nMIP in water suspension as the final product.

2.3. nMIPs characterisation

Fourier transform infrared (FT-IR) spectroscopy was carried out using a Perkin-Elmer Spectrum 2 infrared spectrometer and attenuated total reflectance (ATR) sampling accessory. A few mg of freeze-dried sample was pressed on the ATR crystal using the pressure arm fitted with a large load shoe, resulting in a force gauge reading in the

instrument software of approximately 25. A background measurement was taken in air, and spectra were collected over the wavenumber range 400–4000 cm^{-1} with a resolution of 4 cm^{-1} and 4 scans-to-average. Ultraviolet/visible (UV/vis) spectroscopy was carried out using a Thermo Scientific Evolution 201 UV-Visible Spectrophotometer and a quartz cuvette (path length 1 cm). Deionised water was used as the background measurement, and absorbence was measured over the wavelength range 200 – 1000 nm with a data interval of 1 nm, scan speed of 1500 $nm(min)^{-1}$, and integration time of 0.04 s. Solids content was measured by weighing the mass of a glass vial containing nMIPs suspension (approximately 15 mL) before and after freeze-drying using a Buchi Lyovapor L-200 Freeze Dryer with vacuum pressure set to 0.75 mbar. Before scanning electron microscope (SEM) imaging, samples were dried onto either a Si wafer or the working electrode of a screen-printed electrode (SPE), and dried either at room temperature (19 – 22 °C, approximately 90 – 120 min drying time) or in an oven at 65 °C (approximately 30 min drying time). Before nMIPs deposition, the Si wafers had been rinsed with deionised water, followed by acetone, and then dried with a gentle stream of N_2 (g). The substrates with dry nMIPs were then mounted on aluminium stubs with adhesive carbon tape, and sputter coated with gold using a Polaron SEM Coating System with a coating time of 30 s, and voltage and current of 800 V and 5 mA, respectively. Images were collected with a Supra 40VP from Carl Zeiss Ltd., using a secondary electron detector, acceleration voltage of 2 kV, and working distance of 5.2 mm. Where applicable, particle sizes were analysed using MATLAB R2019a with bespoke code. Filters were applied in the code to remove objects below 30 pixel in area, and above 0.9 in eccentricity, which served to disregard noisy pixels and agglomerated particles, respectively.

2.4. Heat transfer measurements

For studies in aqueous buffer solutions, a master solution of 10 mM creatinine in 0.01 M PBS was made up, and then diluted to the desired concentration ranges. For studies in plasma, a master batch of approximately 0.1 M creatinine was made up in 0.01 M PBS, which was then added blood plasma diluted with 0.01 M PBS (20% v/v plasma) in order to give the desired concentration. The graphite working electrode (WE; diameter = 3.1 mm) of a disposable SPE was used to provide a substrate for supporting the nMIPs in the measurement cell. The SPEs were fabricated as has previously been described [23]. Such SPEs were originally designed to provide a cheap, disposable means of performing electrochemical measurements. However, they have also been shown to be effective substrates for HTM in several instances [21, 24, 25]. In some cases, such SPEs have been electrochemically modified prior to HTM measurements [21, 24], but in this case the WE was used simply to provide a well-defined area for simple drop-casting (with the reference and counter electrodes remaining bare and unused). Specifically, a 10 μL droplet of the nMIPs-in-water suspension obtained directly from the synthesis was pipetted onto the WE of an SPE and allowed to dry at room temperature (19 – 22 °C, approximately 90 – 120 min drying time). A square segment of the SPE with the coated WE at its centre was then placed into the sample chamber of a bespoke, additively manufactured flow cell. The flow cell was produced via stereolithography (SLA) printing and was of a design previously described in literature [21, 25]. Briefly, the unit consisted of: a flow cell with three interior tubes leading to a central sample chamber, two of which act as inflow and outflow for liquid injection, the third allowing insertion of a wire thermocouple; a copper block/heat sink which could be screwed onto the cell; a 22 Ω resistance heater screwed to the exterior of the heat sink and connected to an external power source and PID temperature controller; and an inert substrate (e.g. gold-coated Si wafer) to support the SPE in the sample chamber, plus a rubber O-ring that rests on the SPE, both of which combine to seal the sample chamber upon assembly of the unit. An illustration of the assembled unit is shown in Fig. 1.

Before measurements, a single thermocouple was inserted into the sample chamber through the perpendicular inflow pipe in order to measure the sample temperature (T_2). The tip of the thermocouple was suspended approximately 1.7 mm above the surface of the substrate. A second thermocouple was inserted into the copper heat sink to measure its temperature (T_1). The PID device had previously been optimised through tuning experiments to reduce noise in values of R_{th} measured for the specific cell. The heater was then set to maintain the copper block (T_1) at a temperature of 37 °C during the course of measurement, with the temperatures of the copper block (T_1) and the sample chamber interior (T_2) set to be measured continuously at a sampling rate of 1 Hz. Throughout measurement, the whole assembly was kept in an incubator (VWR INCU-line Cool) maintaining a temperature of 20 °C in order to minimise changes in environmental temperature which could increase the uncertainty in HTM measurements.

Before measurement, either PBS, or the first analyte solution, was injected into the sealed cell, with care being taken to eliminate any bubbles in the sample chamber or ducting as these can unpredictably change the measured R_{th}. The measurement was then commenced. After a 45 min dwell time of the sample in the chamber, the first/next analyte solution was injected into the flow cell at a rate of 250 $\mu L\ min^{-1}$ over the course of 12 min, thereby purging the cell of its previous contents and leaving only the desired analyte solution. After a further 30 min dwell time, the next analyte solution was injected. This process was repeated until all solutions had been measured. This procedure was used for all HTM measurements described here, apart from measurements made using competitor molecules to creatinine, in which case an additional injection of blank PBS solution (with no subsequent dwell time) was carried out between each analyte solution in order to ensure that all of the previous analyte molecule had been removed from the sample cell. For each sample, a mean and standard deviation were taken for 10 min worth of measurements in the period immediately before injection of the next analyte solution.

3. Results and discussion

The nMIPs were fabricated as detailed in the experimental section. We first turn to their characterisation.

3.1. nMIPs characterisation

3.1.1. Spectroscopic characterisation

FT-IR spectroscopy was performed on the freeze-dried nMIPs to assess their chemical composition. The corresponding spectrum is shown in Fig. 3A, with details of the labelled peaks summarised within Table 1. In general, the spectrum was comparable to spectra for PNIPAM found in the literature, [26, 27] although the broad peak centred at approximately 3180 cm^{-1} obscured some additional peaks which should be apparent for the polymer. This broad peak is assumed to be physisorbed water which remains on the hydrophilic polymer after freeze-drying. In addition to the PNIPAM absorption peaks, several peaks at approximately 1000 cm^{-1} and below were observed; these are not consistent with any of the organic components of the polymer, but are similar in position and intensity to absorptions seen when PNIPAM is dried with physisorbed phosphate [28]. This is unsurprising, since phosphate ions are present in the PBS solution used repeatedly during solid-phased templating, and would be expected to remain in the material upon freeze-drying if they had not been washed fully from the glass beads before nMIP synthesis. Although the presence of phosphate is not expected to be an issue for the application of the nMIPs in sensing, purer material could be obtained through dialysis in deionised water if so desired. There are no obvious absorption peaks representing the other organic components expected to form part of the polymer (i.e. BIS and CTP), but this is probably due to the fact that they are expected to form a relatively small fraction of the material, hence their absorption peaks could obscured by those of the PNIPAM, and/or may not be discernible in this measurement configuration (i.e. because of the short path length

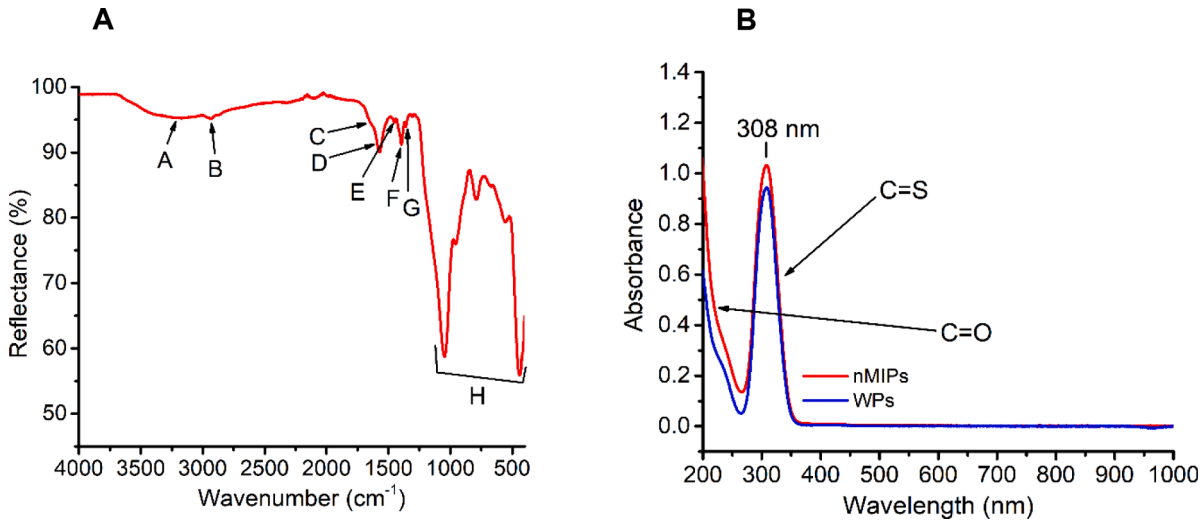

Fig. 3. (A) FT-IR spectrum of the nMIPs obtained after freeze-drying. Peaks labelled A – G can be assigned to vibrations expected for PNIPAM, and the peaks collectively labelled H arise from phosphate left in the material after drying (see Table 1); (B) UV/vis spectra of nMIPs and WPs. The spectra show peaks at 308 nm corresponding to the thiocarbonyl group of the iniferter agent, and the shoulder of a peak corresponding to carbonyl groups in the polymer backbone.

Table 1
FT-IR peak positions and assignments for the creatinine imprinted nMIPs.

Peak label	Peak wavenumber/cm^{-1}	Assignment
A	3180 (broad)	H_2O
B	2935	sp^3 C-H[26]
C, D	1640 (shoulder), 1573	Amide[26]
E	1452	-$C(CH_3)_2$ symmetric deformation[26]
F, G	1394, 1359	-$C(CH_3)_2$ antisymmetric deformation[26]
H	1100 – 400	Phosphate[28]

inherent to spectroscopy carried out using an ATR accessory). Overall, from the FT-IR data it can be concluded that a material consisting mainly of PNIPAM has been synthesised.

A UV/vis absorption spectrum for the obtained nMIPs is shown in Fig. 3B. The peak centred at 308 nm corresponds to the π→π* electronic transition of the thiocarbonyl group in the iniferter agent [29], which is expected to remain as part of the structure of the obtained polymers. The large peak extending below the measured minimum wavelength of 200 nm is assigned to the carbonyl group of the poly(amide). Also shown is a spectrum for a sample taken from the last room temperature washing step of the synthesis, labelled Washing Polymers (WPs). It can be seen that the absorbence at 308 nm of the WPs is only slightly lower than that of the nMIPs; the ratio of absorbances nMIPs:WPs at 308 nm was found to be 0.91. As per the Beer-Lambert law, absorbence is directly proportional to concentration when the measured path length and absorptivities are the same (as in this case), hence it can be inferred that the WPs contained 91% of the same polymer content as the obtained nMIPs. This demonstrates that substantial polymer material is still being lost during the final room temperature washing steps of the synthesis, at which point the only remaining polymer was intended to be bound to the glass beads (and hence not removable by the wash). However, from this data alone it cannot be concluded whether the WPs represent unwanted, non-imprinted polymer, or usable MIP.

3.1.2. Solids concentration

The solids concentration in the obtained nMIPs suspension was found by measuring the mass of sample in a glass vial before and after freeze-drying. Through using this methodology, the solids concentration in suspension was found to be (206 ± 6) μg mL^{-1}, where the uncertainty has been propagated from uncertainty in the mass balance used. In turn, this can be used to calculate the mass of solid obtained per mass of glass bead template, which was found to be (104 ± 3) μg g^{-1}. However, it should be noted that these are likely overestimates of the nMIPs concentration; some contribution to the mass of the solid obtained by freeze drying will arise from both physisorbed water, and salts found by IR spectroscopy to remain from the PBS solutions (although this is difficult to quantify). By the same method, the solids concentration in the suspension of WPs was found to be (86 ± 5) μg mL^{-1}, which is substantially less than suggested by UV spectroscopy, but nonetheless still represents a significant mass loss during the final washing step. Canfarotta et al. report a minimum yield of approximately 200 μg g^{-1} (μg nMIPs per g beads) from their synthesis [15], double that obtained here. According to their "troubleshooting" guide, Canfarotta et al. suggest that the cause of the lower than expected yields could be low amounts of immobilised template on the solid phase, or incomplete elution of the nMIPs from the solid phase [15]. However, from the measured solids concentration of WPs and the results of Section 3.1.1, it seems likely that unintended loss of nMIPs during washing is the most significant cause of the low yield of nMIPs in this modified synthesis.

3.1.3. SEM

When dried on a Si wafer in an oven at 65 °C, the nMIPs appear as discrete, roughly spherical particles; see Fig. 4A. Automated computational image analysis can be used to measure the sizes of the particles, with the resulting size distribution shown in Fig. 4B. The particle diameters appear to follow lognormal distribution, with a mode diameter of approximately 120 nm, and an arithmetic mean diameter of (150 ± 47) nm. A sample of WPs imaged in the same manner showed particles of a similar nature and size (see SI), providing further evidence that polymer is unintentionally lost during the final washing step of the synthesis. Intriguingly, when the nMIP solution was dried on a Si wafer at room temperature, the nMIPs appeared to form a film rather than remaining as discrete particles; see Fig. 4C. This is not necessarily unusual behaviour, since colloidal polymer particles often form a film upon drying under the right conditions (e.g. latex based paints), although it might indicate a low degree of crosslinking within the polymer. However, another possible cause of this phenomenon is the complex phase behaviour of PNIPAM, which is known to possess an aqueous Lower Critical Solution Temperature (LCST) of approximately 32 °C; above this temperature, the polymer becomes insoluble, expelling water and forming discrete globules or otherwise undergoing phase separation. [30] As such, it is difficult to state conclusively whether the particles observed in Fig. 4 represent discrete nanoparticles which form a film upon drying, or polymer chains which agglomerate into globules above

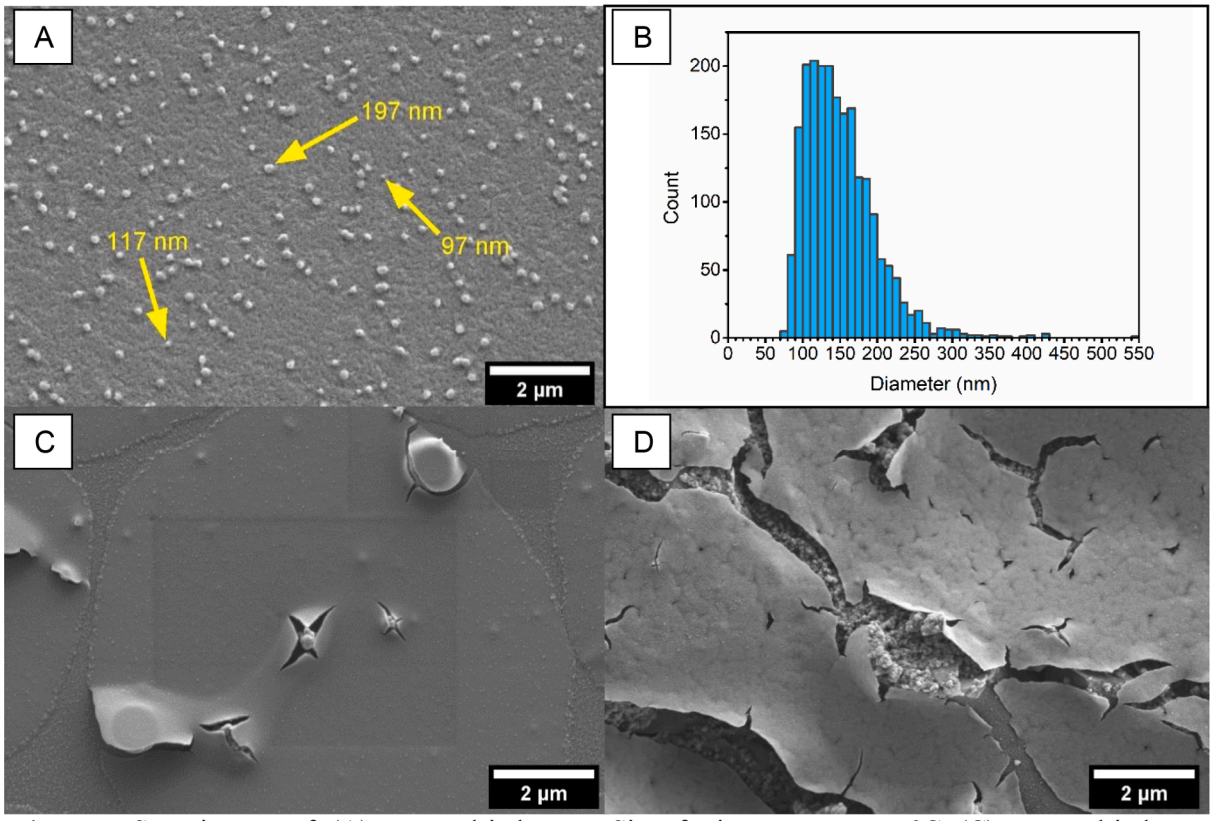

Fig. 4. SEM images of: (A) nMIPs dried onto a Si wafer in an oven at 65 °C; (C) nMIPs dried onto a Si wafer at room temperature; and (D) the WE of an SPE onto which the nMIPs solution was dried at room temperature. The diameter distribution of the particles observed in (A) is shown in (B).

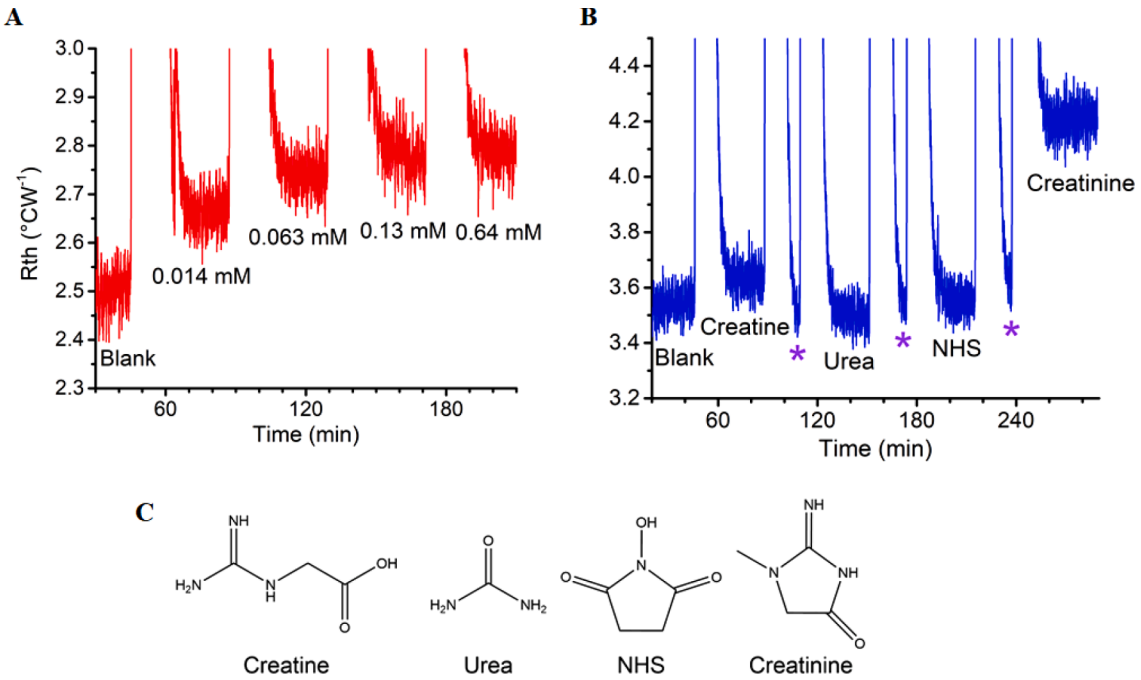

Fig. 5. (A) R_{th} versus time for the creatinine imprinted nMIPs upon injection of increasingly concentrated creatinine solutions; (B) R_{th} versus time upon sequential injection of approximately 0.6 mM creatinine competitor solutions, followed by a final injection of approximately 0.6 mM creatinine solution; (C) chemical structures of the competitor molecules studied in comparison to creatinine. In (B), the three injections marked by asterisks correspond to purging of the cell with blank PBS solution between each test molecule solution injection.

the LCST. Dynamic Light Scattering (DLS) measurements carried out on the solution were inconclusive, as the obtained data was low quality, with "expert advice" in the instrument software indicating the presence of large particles, likely fragments of glass noted by Canfarotta et al. to occur frequently in their procedure [15]. Nonetheless, for the purposes of this work the sample will be assumed to be formed of nMIPs which form a polymer film upon drying. The working electrode of an SPE was used to provide a substrate for supporting the nMIPs during HTM measurements. An SEM image of the nMIPs dried at room temperature on an SPE is shown in Fig. 4D. As with samples dried on a Si wafer, under these conditions, the nMIPs appear to have formed a film on the electrode surface rather than remaining as discrete particles. Despite the lack of discrete particles, drying the nMIPs at room temperature was investigated rather than oven heating as it was unknown what effect increased temperature would have on the polymer (and insufficient material was available for thermal analysis).

3.2. Heat transfer measurements

Despite their low concentration in solution, and their tendency to form a film on the SPE surface, the drop-cast nMIPs were found to be effective for sensing creatinine in PBS buffer solution. Fig. 5A shows the raw HTM data (R_{th} versus time) for the nMIPs on the SPEs. In a solution of PBS, the thermal resistance stabilised at an R_{th} of (2.51 ± 0.03) °C W^{-1}. Upon the sequential addition of increasingly concentrated creatinine solutions, the R_{th} increased up to a maximum of (2.79 ± 0.03) °C W^{-1} at a creatinine concentration of 0.64 mM, an increase of (0.28 ± 0.05) °C W^{-1}, or (11 ± 1)%. An increase in the thermal resistance of a system containing MIPs particles arises due to the binding of molecules from solution, which reduces heat flux through the MIPs layer (e.g. by blocking of pores and channels) [20]. These data demonstrate that the synthesised nMIPs have successfully been imprinted with creatinine.

The selectivity of the nMIPs towards creatinine binding was investigated by measuring their R_{th} upon exposure to "competitor" molecules which are chemically and/or structurally similar to creatinine. Fig. 5B shows R_{th} versus time for the nMIPs when sequentially exposed to approximately 0.6 mM solutions of such competitor molecules. For urea and N-hydroxysuccinimide (NHS), changes in R_{th} of (−1.4 ± 1.3)% and (0.07 ± 1.05)% were measured, respectively; these are changes are small and close to or within the measured uncertainties, hence it can be concluded that these competitor molecules show little to no binding to the nMIPs. By contrast, an increase of (0.08 ± 0.06) °CW^{-1}, or (2.4 ± 1.4)%, was observed upon exposure to creatine. However, this is significantly lower than the increase of (0.66 ± 0.06) °CW^{-1}, or (19 ± 1)%, which occurred when the same system was subsequently exposed to a similar concentration of creatinine. Overall, it can be concluded that the synthesised nMIPs bind creatinine selectively, although it must be noted that the presence of large concentrations of creatine in a sample would be expected to cause misleading HTM results. Furthermore, the fact that a similarly significant change in R_{th} in the presence of creatinine is still observed in Fig. 5B after almost twice the number of injection steps as in Fig. 5A implies that the nMIPs are stable on the SPE substrate and are not washed away during analyte injections.

A plot of absolute change in R_{th}, ΔR_{th}, versus creatinine concentration is shown in Fig. 6. There is clearly a nonlinear relationship between creatinine concentration and the observed ΔR_{th} of the system, with ΔR_{th} initially increasing rapidly as creatinine is added, then increasing less rapidly over intermediate concentrations, before finally beginning to plateau, presumably as the creatinine binding sites on the nMIPs become saturated. The nonlinear relationship between R_{th} and analyte concentration is typical of HTM measurements, with the data found here similar to the curves previously reported when MIPs[19, 31] or antibodies[21] have been used to bind a target molecule and cause a change in thermal resistance. In the SI, HTM data for the WP sample are also shown. The WP HTM results were similar to those of the obtained nMIPs; it can therefore be concluded that the polymer material being unintentionally lost in cold washing is of similar quality for sensing as that obtained from final, hot washing step of the synthesis. It can therefore be concluded that this lower-cost, modified method is slightly wasteful and could be optimised further but can indeed be used to make nMIPs imprinted for creatinine which are suitable for HTM measurements.

Previous HTM literature has tended to fit R_{th} versus concentration data with equations of the type shown in Eq. (2), [19, 21] i.e. the pre-loaded "Dose-Response" (DR) nonlinear fitting equations in

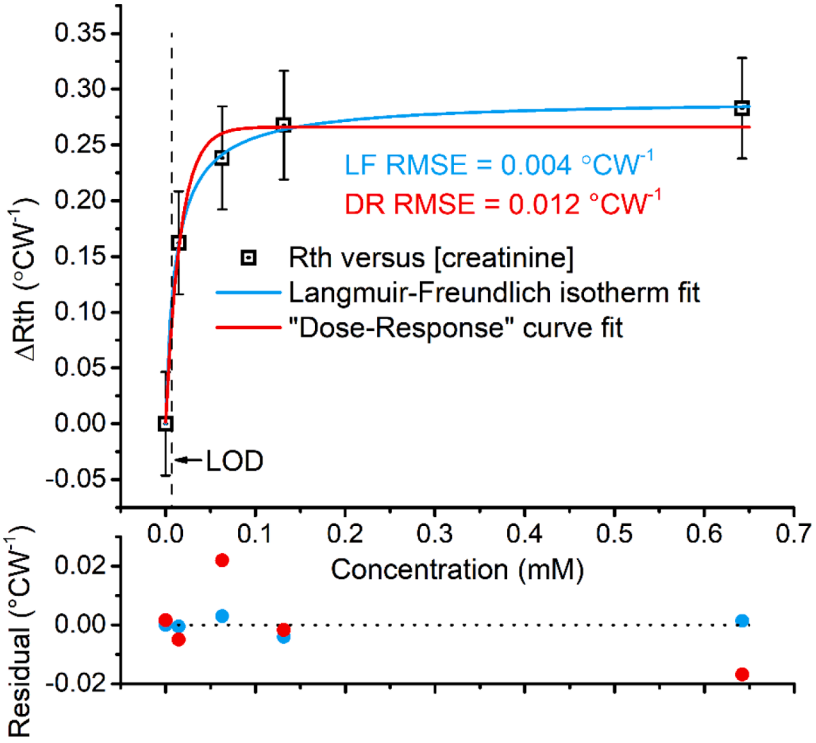

Fig. 6. ΔR_{th}, versus creatinine concentration for the synthesised nMIPs. The data show a nonlinear relationship which is described better using a fit derived from the Langmuir-Friedrich isotherm (Eq. (3)) than the "Dose-Response" curves (Eq. (2)) that have been used in the past for similar data. This is evidenced by smaller residuals and correspondingly smaller RMSE for the LF fit compared to the DR fit. The limit-of-detection (LOD) derived using the LF fit is illustrated with the dashed line. The error bars represent the standard deviation over 10 min of measurements made at each concentration.

OriginLab graphing software. In Eq. (2), y is taken as the ΔR_{th} data, x is the analyte concentration, and A_1, A_2, x_0, and p are constants. However, while such equations can fit the data well, they do not contain any information about the adsorbent (in this case, MIPs). By contrast, the Langmuir-Freundlich isotherm suggested for MIPs characterisation by Umpleby et al. [32] contains information about the adsorbent, including the number of binding sites and the binding affinity. More specifically, for a heterogeneous system, the LF isotherm describes the equilibrium concentration of bound adsorbate (y) in terms of: the total number of binding sites (N_t); a constant, a, which is related to the median binding affinity of the adsorbate on the adsorbent; a heterogeneity index, m, which is related to the heterogeneity of the adsorbate binding sites; and the concentration of adsorbate in solution, x. This is shown in Eq. (3). With the assumption that ΔR_{th} is directly proportional to the equilibrium concentration of bound adsorbate, Eq. (3) can be fitted directly to the ΔR_{th} data and compared to Eq. (2). The two fits can be seen in Fig. 6, and, from inspection of the fitted curves and the corresponding residuals, it is clear that the LF isotherm is a better fit for the data than the DR curve. This is further evidenced by the lower root-mean-squared-error (RMSE) for the LF fit than the DR fit; these were 0.004 °C W^{-1} and 0.012 °C W^{-1}, respectively. The limit-of-detection (LOD) was estimated by fitting a line of the form $y = bx + c$ to the initial section (i.e. 0 mM – 0.004 mM) of the LF curve and using the fitted gradient, b, to calculate the LOD as per the 3σ method. More specifically, the standard deviation of the lowest measured concentration was multiplied by three and divided by the slope (b) of the fitted straight line. This gave a LOD of (7.0 ± 0.5) μM, where the uncertainty in LOD has been propagated from the uncertainty in the fitted value of b. The position of the LOD relative to the data is illustrated in Fig. 6.

$$y = A_1 + \frac{A_2 - A_1}{1 + 10^{(log x_0 - x)p}} \tag{2}$$

$$y = \frac{N_t a x^m}{1 + a x^m} \tag{3}$$

With healthy serum creatinine concentrations covering the range 5 – 12 ppm (approximately 0.04 – 0.1 mM) [16], significantly higher than the estimated LOD of 7 μM, it is clear that the as-synthesised nMIPs are sensitive enough to be used in HTM for detection of clinically relevant concentrations of serum creatinine, even when simply drop-cast onto the WE of an SPE. However, the nMIPs cannot be concluded to useful for clinical application on the basis of the measurements in PBS solution alone, since real plasma samples are expected to contain a variety of competitor molecules and other interferents. To prove the utility of the nMIPs in real samples, further HTM measurements were carried out in PBS-diluted "blank" blood plasma, which is assumed to contain a healthy baseline creatinine concentration, and plasma spiked with additional creatinine to give a concentration increase typical of a real clinical measurement. Dilution with PBS solution was necessary to bring the change in creatinine concentration into the range in which the R_{th} of the nMIPs changes rapidly with creatinine, but above the LOD shown in Fig. 6. More specifically, the blood plasma was spiked with 0.1 M creatinine solution (on the order of μL) to give a concentration of approximately 0.05 mM (50 μM) in the undiluted plasma, which is in the range of clinically relevant changes in creatinine concentration as described by the BMJ [5]. Diluting this plasma sample with PBS solution to 20% (v/v) gives a creatinine concentration of approximately 10 μM, which is in the optimum measurement range for detection and above the calculated LOD of 7 μM. As can be seen in Fig. 7, exposing the nMIPs to the creatinine-spiked plasma solution after the blank plasma solution led to an increase in R_{th} of (0.11 ± 0.07) °CW^{-1}, which is of a similar order of magnitude as the ΔR_{th} seen in pure buffer solution (e.g. in Fig. 6). These data show that the SPE-supported nMIPs can be used in HTM to detect clinically relevant changes in creatinine concentration in real blood samples.

The red crosses in Fig. 7 represent brief periods of increased noise as the cell temperature restabilised after the door to the incubator had been opened (which let in cold air) in order to allow the cell to be checked for bubbles. Indeed, bubble formation was found to occur more readily in plasma and PBS-diluted plasma samples than in PBS solutions, which can be attributed to the ability of blood plasma proteins to stabilise foams [33]. It is for this reason that full dose-response data could not be collected for plasma samples; multiple injections into the flow cell consistently led to bubbles large or numerous enough to invalidate the measurement run. This is an issue which would have to be resolved

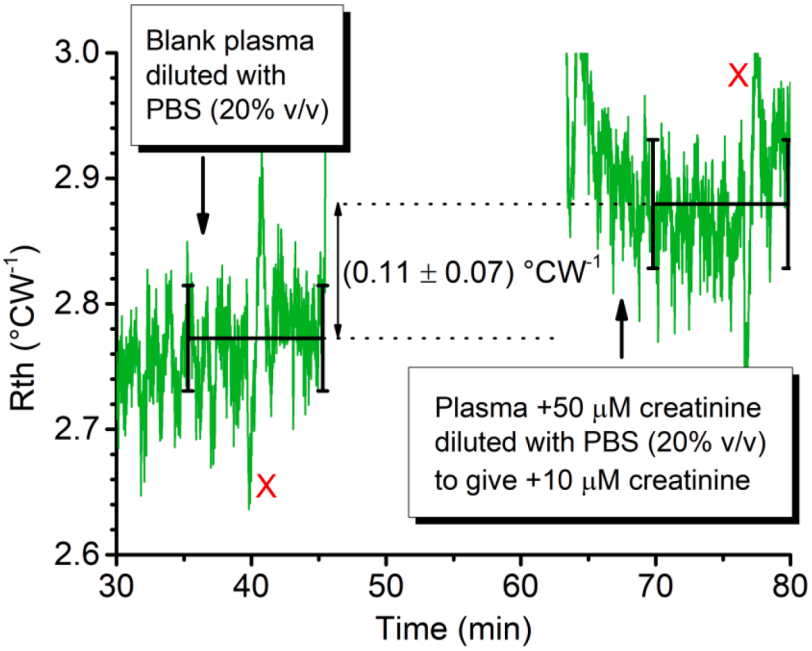

Fig. 7. HTM data for a blank PBS solution, blank plasma solution diluted with PBS (20% v/v), and a 50 μM creatinine-spiked plasma solution diluted with PBS (20% v/v) (i.e. a 10 μM spiked increase in creatinine taking into account dilution). The red crosses indicate brief periods of increased uncertainty after the incubator was opened to check the cell for bubbles. The lines and error bars represent the means and standard deviation of ten minutes of measurements.

before the set-up described here could be applied for real clinical use. Possible solutions could include changing the ducting to the sample cell to reduce the likelihood of bubble formation or designing a new cell with a built-in means of quickly removing bubbles during measurement without significantly disturbing the system.

4. Conclusion

We have shown that PNIPAM nMIPs imprinted for creatinine can be produced using a simplified version of the aqueous synthesis described previously by Canfarotta et al. [15]. Simple drop-casting of PNIPAM nMIPs solution onto a cheap, disposable SPE produced a film when dried at room temperature rather than the desired layer of discrete nanoparticles. However, the platform was nonetheless shown to be effective for HTM sensing of creatinine in buffer solutions, with a LOD of (7.0 ± 0.5) μM calculated using a fitted Langmuir-Freundlich isotherm and the 3σ method. The nMIPs were found to bind creatinine selectively versus several similar molecules and were subsequently shown to be able to detect clinically relevant changes in creatinine concentration in complex blood plasma samples.

However, for the application to real clinical situations, it is likely that further optimisation would be required. For example, a synthesis different to that described here would be needed to produce more effective nMIPs; the use of a monomer other than NIPAM, and/or a larger amount of cross-linker relative to monomer could avoid the formation of a polymer film on the substrate surface and the associated reduction in surface area compared to a discrete nanoparticle layer. Similarly, a HTM system would need to be used which could mitigate for the increased tendency for problematic bubble formation observed in blood plasma samples. Nonetheless, it can be concluded that the combination of simple drop-casting of creatinine-imprinted nMIPs onto disposable SPEs, and subsequently using HTM as a readout method, provides a promising alternative platform for clinical serum creatinine testing which merits further investigation.

Declaration of Competing Interest

The authors declare that they have no known competing financial interests or personal relationships that could have appeared to influence the work reported in this paper.

Supplementary materials

Supplementary material associated with this article can be found, in the online version, at doi:10.1016/j.talo.2022.100087.

References

[1] R.D. Perrone, N.E. Madias, A.S. Levey, Serum creatinine as an index of renal function - new insights into old concepts, Clin. Chem. 38 (10) (1992) 1933–1953.
[2] M. Wyss, R. Kaddurah-Daouk, Creatine and creatinine metabolism, Physiol. Rev. 80 (3) (2000) 1107–1213.
[3] S. Herget-Rosenthal, A. Bokenkamp, W. Hofmann, How to estimate GFR - serum creatinine, serum cystatin C or equations? Clin. Biochem. 40 (3–4) (2007) 153–161.
[4] V. Sirolli, L. Pieroni, L. Di Liberato, A. Urbani, M. Bonomini, Urinary Peptidomic Biomarkers in Kidney Diseases, Int. J. Mol. Sci. 21 (1) (2020) 15.
[5] Assessment of elevated creatinine, 2020. https://bestpractice.bmj.com/topics/en-gb/935. (Accessed 2021.08.27 2021).
[6] P. Delanaye, E. Cavalier, H. Pottel, Serum Creatinine: Not So Simple!, Nephron 136 (4) (2017) 302–308.
[7] R. Canovas, M. Cuartero, G.A. Crespo, Modern creatinine (Bio)sensing: Challenges of point-of-care platforms, Biosens. Bioelectron. 130 (2019) 110–124.
[8] A. Rico-Yuste, S. Carrasco, Molecularly Imprinted Polymer-Based Hybrid Materials for the Development of Optical Sensors, Polymers 11 (7) (2019) 44.
[9] J.C. Yang, S.W. Hong, J. Park, Improving Surface Imprinting Effect by Reducing Nonspecific Adsorption on Non-Imprinted Polymer Films for 2,4-D Herbicide Sensors, Chemosensors 9 (3) (2021) 10.
[10] J.W. Lowdon, H. Dilien, P. Singla, M. Peeters, T.J. Cleij, B. van Grinsven, K. Eersels, MIPs for commercial application in low-cost sensors and assays - An overview of the current status quo, Sens. Actuator B-Chem. 325 (2020) 19.
[11] G. Selvolini, G. Marrazza, MIP-Based Sensors: Promising New Tools for Cancer Biomarker Determination, Sensors 17 (4) (2017) 19.
[12] R.D. Crapnell, A. Hudson, C.W. Foster, K. Eersels, B. van Grinsven, T.J. Cleij, C. E. Banks, M. Peeters, Recent Advances in Electrosynthesized Molecularly Imprinted Polymer Sensing Platforms for Bioanalyte Detection, Sensors 19 (5) (2019) 28.
[13] D. Refaat, M.G. Aggour, A.A. Farghali, R. Mahajan, J.G. Wiklander, I.A. Nicholls, S. A. Piletsky, Strategies for Molecular Imprinting and the Evolution of MIP Nanoparticles as Plastic Antibodies-Synthesis and Applications, Int. J. Mol. Sci. 20 (24) (2019) 21.
[14] S. F.C. Canfarotta, A. Piletsky, Nano-sized Molecularly Imprinted Polymers as Artificial Antibodies, in: W.S. Kutner, S. P. (Eds.), Molecularly Imprinted Polymers For Analytical Chemistry Applications, Royal Society of Chemistry, 2018, pp. 1–27.
[15] F. Canfarotta, A. Poma, A. Guerreiro, S. Piletsky, Solid-phase synthesis of molecularly imprinted nanoparticles, Nat. Protoc. 11 (3) (2016) 443–455.
[16] S.N.M Prabhu, C S, C.P Gooneratne, A.S Davidson, G Liu, Molecularly Imprinted Polymer-based detection of creatinine towards smart sensing, Medical Devices & Sensors 3 (6) (2020) 1–17.
[17] T.J. Li, P.Y. Chen, P.C. Nien, C.Y. Lin, R. Vittal, T.R. Ling, K.C. Ho, Preparation of a novel molecularly imprinted polymer by the sol-gel process for sensing creatinine, Anal. Chim. Acta 711 (2012) 83–90.
[18] M. Hassanzadeh, M. Ghaemy, An effective approach for the laboratory measurement and detection of creatinine by magnetic molecularly imprinted polymer nanoparticles, New J. Chem. 41 (6) (2017) 2277–2286.
[19] R.D. Crapnell, F. Canfarotta, J. Czulak, R. Johnson, K. Betlem, F. Mecozzi, M. P. Down, K. Eersels, B. van Grinsven, T.J. Cleij, R. Law, C.E. Banks, M. Peeters, Thermal Detection of Cardiac Biomarkers Heart-Fatty Acid Binding Protein and ST2 Using a Molecularly Imprinted Nanoparticle-Based Multiplex Sensor Platform, ACS Sens 4 (10) (2019) 2838–2845.
[20] B. van Grinsven, K. Eersels, M. Peeters, P. Losada-Perez, T. Vandenryt, T.J. Cleij, P. Wagner, The Heat-Transfer Method: A Versatile Low-Cost, Label-Free, Fast, and User-Friendly Readout Platform for Biosensor Applications, ACS Appl. Mater. Interfaces 6 (16) (2014) 13309–13318.
[21] R.D. Crapnell, W. Jesadabundit, A.G.M. Ferrari, N.C. Dempsey-Hibbert, M. Peeters, A. Tridente, O. Chailapakul, C.E. Banks, Toward the Rapid Diagnosis of Sepsis: Detecting Interleukin-6 in Blood Plasma Using Functionalized Screen-Printed Electrodes with a Thermal Detection Methodology, Anal. Chem. 93 (14) (2021) 5931–5938.
[22] S. Beyazit, B.T.S. Bui, K. Haupt, C. Gonzato, Molecularly imprinted polymer nanomaterials and nanocomposites by controlled/living radical polymerization, Prog. Polym. Sci. 62 (2016) 1–21.
[23] C.W. Foster, J.P. Metters, D.K. Kampouris, C.E. Banks, Ultraflexible Screen-Printed Graphitic Electroanalytical Sensing Platforms, Electroanalysis 26 (2) (2014) 262–274.
[24] O. Jamieson, T.C.C. Soares, B.A. de Faria, A. Hudson, F. Mecozzi, S.J. Rowley-Neale, C.E. Banks, J. Gruber, K. Novakovic, M. Peeters, R.D. Crapnell, Screen Printed Electrode Based Detection Systems for the Antibiotic Amoxicillin in Aqueous Samples Utilising Molecularly Imprinted Polymers as Synthetic Receptors, Chemosensors 8 (1) (2020) 14.
[25] S. Casadio, J.W. Lowdon, K. Betlem, J.T. Ueta, C.W. Foster, T.J. Cleij, B. van Grinsven, O.B. Sutcliffe, C.E. Banks, M. Peeters, Development of a novel flexible polymer-based biosensor platform for the thermal detection of noradrenaline in aqueous solutions, Chem. Eng. J. 315 (2017) 459–468.
[26] Y. Maeda, T. Higuchi, I. Ikeda, Change in hydration state during the coil-globule transition of aqueous solutions of poly(N-isopropylacrylamide) as evidenced by FTIR spectroscopy, Langmuir 16 (19) (2000) 7503–7509.
[27] B.J. Sun, Y.A. Lin, P.Y. Wu, Structure analysis of poly(N-isopropylacrylamide) using near-infrared spectroscopy and generalized two-dimensional correlation infrared spectroscopy, Appl. Spectrosc. 61 (7) (2007) 765–771.
[28] Z. Cao, Y.Y. Chen, D. Li, J.F. Cheng, C.L. Liu, Fabrication of Phosphate-Imprinted PNIPAM/SiO2 Hybrid Particles and Their Phosphate Binding Property, Polymers 11 (2) (2019) 18.
[29] K. Skrabania, A. Miasnikova, A.M. Bivigou-Koumba, D. Zehm, A. Laschewsky, Examining the UV-vis absorption of RAFT chain transfer agents and their use for polymer analysis, Polym. Chem. 2 (9) (2011) 2074–2083.
[30] I. Bischofberger, V. Trappe, New aspects in the phase behaviour of poly-N-isopropyl acrylamide: systematic temperature dependent shrinking of PNiPAM assemblies well beyond the LCST, Sci Rep 5 (2015) 10.
[31] J.W. Lowdon, K. Eersels, R. Rogosic, T. Boonen, B. Heidt, H. Dilien, B. van Grinsven, T.J. Cleij, Surface grafted molecularly imprinted polymeric receptor layers for thermal detection of the New Psychoactive substance 2-methoxphenidine, Sens. Actuator A-Phys. 295 (2019) 586–595.
[32] R.J. Umpleby, S.C. Baxter, M. Bode, J.K. Berch, R.N. Shah, K.D. Shimizu, Application of the Freundlich adsorption isotherm in the characterization of molecularly imprinted polymers, Anal. Chim. Acta 435 (1) (2001) 35–42.
[33] M.O. Raeker, L.A. Johnson, Thermal and functional properties of bovine blood plasma and egg-white proteins, J. Food Sci. 60 (4) (1995) 685–690.